A Non-Destructive Method for Dating Human Remains

Warren K. Lail, David Sammeth, Shannon Mahan, and Jason Nevins

ABSTRACT

The skeletal remains of several Native Americans were recovered in an eroded state from a creek bank in northeastern New Mexico. Subsequently stored in a nearby museum, the remains became lost for almost 36 years. In a recent effort to repatriate the remains, it was necessary to fit them into a cultural chronology in order to determine the appropriate tribe(s) for consultation pursuant to the Native American Grave Protection and Repatriation Act (NAGPRA). Because the remains were found in an eroded context with no artifacts or funerary objects, their age was unknown. Having been asked to avoid destructive dating methods such as radiocarbon dating, the authors used Optically Stimulated Luminescence (OSL) to date the sediments embedded in the cranium. The OSL analyses yielded reliable dates between A.D. 1415 and A.D. 1495. Accordingly, we conclude that the remains were interred somewhat earlier than A.D. 1415, but no later than A.D. 1495. We believe the remains are from individuals ancestral to the Ute Mouache Band, which is now being contacted for repatriation efforts. Not only do our methods contribute to the immediate repatriation efforts, they provide archaeologists with a versatile, non-destructive, numerical dating method that can be used in many burial contexts.

Los restos óseos de varios nativos americanos fueron recuperados al encontrarles en estado de erosión a la orilla de un arroyo en el noreste de Nuevo México. Al ser subsecuentemente almacenados en un museo cercano, los restos se perdieron entre las colecciones por casi 36 años. Recientemente, ante la necesidad de repatriarlos a la tribu de nativos americanos correspondiente, ha sido necesario ubicarles en una cronología cultural, de conformidad con el Acta de Protección y Repatriación de Tumbas de los Nativos Norteamericanos (NAGPRA), para consultar con la tribu o tribus apropiadas. Dado que los restos fueron encontrados en un contexto erosionado, sin artefactos u objetos funerarios, se desconoce su antigüedad. Al haberse pedido que no se utilizaran métodos de datación destructivos, como radiocarbono, los autores utilizaron luminiscencia ópticamente estimulada (OSL) para fechar los sedimentos que se encontraban al interior del cráneo. Los análisis de OSL proveyeron fechas confiables entre 1415 y 1495 d.C. Consecuentemente, concluimos que los restos fueron enterrados poco antes de 1415 d.C., mas no después de 1495 d.C. Nosotros creemos que los restos son ancestros de los miembros de la banda Mouache Ute, a quienes se les ha contactado como parte de las acciones de repatriación. No solo nuestros métodos contribuyen a estos esfuerzos inmediatos de repatriación, éstos proveen a los arqueólogos con un método de datación versátil y no destructivo que puede utilizarse en distintos contextos mortuorios.

During the summer of 1973, human skeletal remains were found eroding in the banks of the Cimarroncito Creek on the historic UU Bar Ranch in Colfax County, New Mexico (Figure 1). A young archaeologist from the adjoining Philmont Scout Ranch hastily recovered the remains and stored them in the Philmont Museum, where they became lost amid the collections for almost 36 years. In 2009, the newly appointed curator of the museum discovered the remains and asked that they be examined at the Research Laboratory of Anthropology at New Mexico Highlands University and that arrangements be made for their reinterment according to law. Among the museum records, only a single page of original field notes documenting the recovery was found. Unfortunately, the position along the creek from which the remains were recovered was not recorded. Loan documentation was completed, and the remains were transferred and housed in our curation facilities until the analysis could begin.

After a cursory examination, we believed the remains to be those of a Native American. Moreover, we observed that the cranium had not been cleaned and was still filled with compacted sediments (Figure 2). We then asked and received permission to conduct a non-destructive analysis of the remains and to repatriate them consistent with the Native American Graves Protection and Repatriation Act (NAGPRA), 25 U.S.C. 3001 et seq. (1990),

https://doi.org/10.7183/2326-3768.1.2.91 Published online by Cambridge University Press



FIGURE 1. The Colfax County study area denoted as green rectangle. Superimposed image with arrow indicating general location of Cimarroncito Creek (view north from Urraca Mesa). Base map courtesy Joe Zebrowski, New Mexico Highlands University. Photo inset by Warren Lail.

and more specifically with the "Final Rule" for disposition of culturally unidentifiable Native American human remains under 43 CFR 10 (2010). The 2010 Final Rule came about because the original act did not address the disposition of culturally unidentifiable remains, which became a growing concern for Native Americans, as well as for museums and other organizations wishing to repatriate such remains.

Repatriation normally begins with a determination of "shared group identity that can be reasonably traced historically or prehistorically between a present-day Indian tribe … and an identifiable earlier group" (43 CFR 10.2[e][1]). Relevant information for making this determination includes geographic region and occupation periods known through archaeological, historical, linguistic, or folkloric evidence (43 CFR 10.2[e][1]). Unfortunately, the prehistory of the Cimarron District is not yet fully understood (Lail 2008). However, under the Final Rule, culturally unidentifiable human remains may be repatriated under relaxed lineage standards. Culturally unidentifiable remains are defined as "human remains and associated funerary objects in museum or Federal agency collections for which no lineal descendant or culturally affiliated Indian tribe or Native Hawaiian organization has been identified" (43 CFR 10.2[e][2]). Under the Final Rule, the remains may be repatriated to a tribe that is "recognized as aboriginal to the area from which the human remains were removed" (43 CFR 10.10[c][1][ii]). Because no artifacts or associated funerary objects were recovered with the remains, it was impossible to fit them into a regional cultural chronology (Table 1), which in turn made it difficult to determine the proper tribe(s) for consultation regarding repatriation. Although radiocarbon dating would place the remains within an occupational time frame, it would require the destruction of a small piece of bone,

https://doi.org/10.7183/2326-3768.1.2.91 Published online by Cambridge University Press

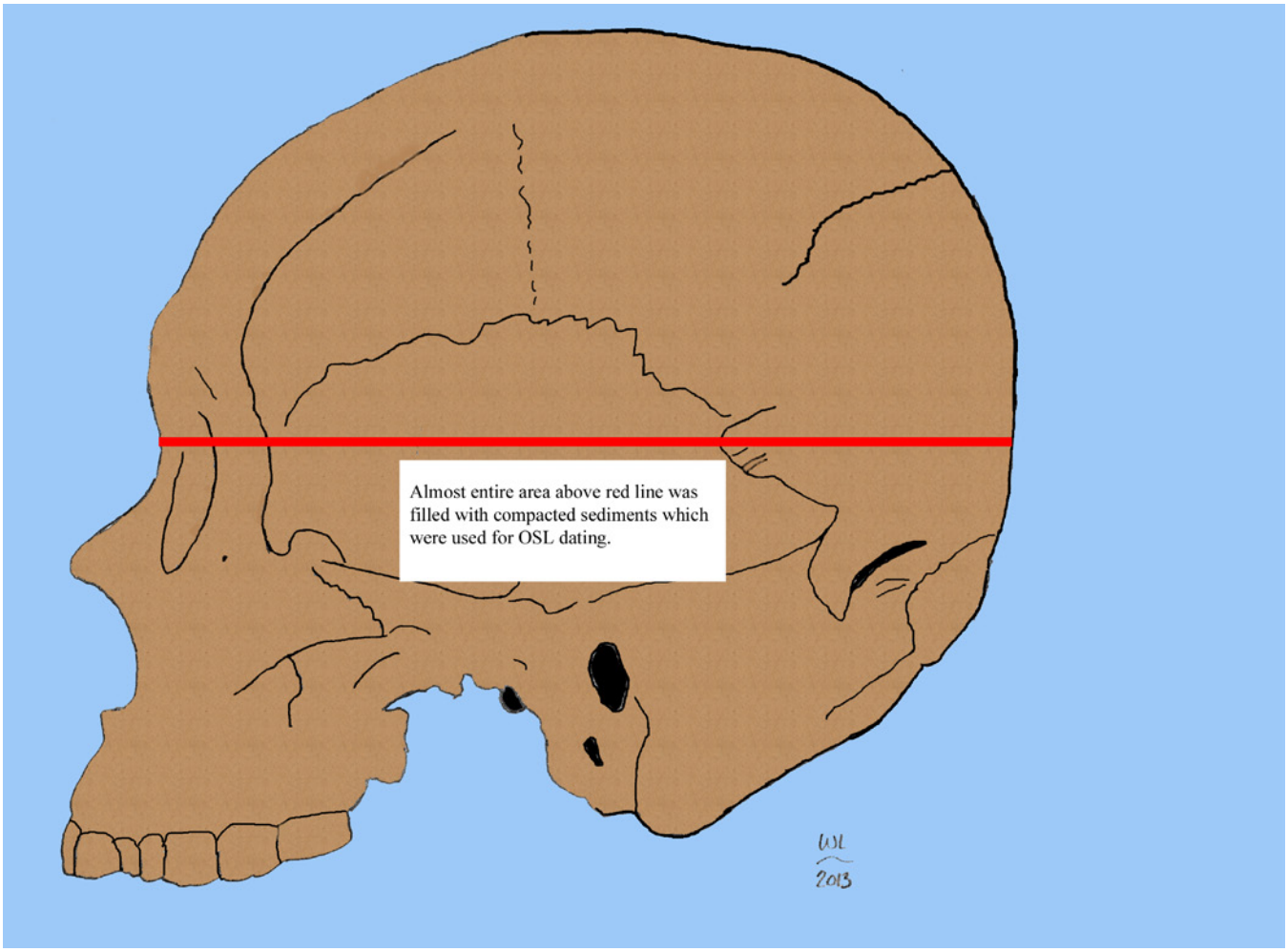


FIGURE 2. Much of the cranium was filled with compacted sediments which were used for OSL testing. Illustration by Warren Lail.

a practice some Native American tribes oppose, and something we were asked to avoid.

METHODS

Bioarchaeological Methods

Our assessments of sex, age at death, and ancestry followed the common protocols of bioarchaeology and forensic anthropology for skeletonized human remains (see Buikstra and Ubelaker 1994; Burns 2013; France 1998; Krogman 1962; Snow 1982). First, we determined that more than one individual was represented; the remains consisted of an intact soil-reddened skull with mandible, together with a second disarticulated maxilla and other bones and elements exhibiting a different coloration. Accordingly, the minimum number of individuals represented was two (MNI = 2). Although we intend to repatriate all of the remains, only the intact soil-reddened skull is the focus of this paper.

Assessment of Sex

We used both anthroposcopic and osteometric evaluations of the cranium and mandible to assess the decedent's sex. When both methods are employed, the most accurate results are obtained (Berg 2008; Ramsthaler et al. 2007). Anthroposcopically, we observed that the cranium exhibited overall ruggedness with smooth muscle markings, an intermediate brow-ridge, a slanted frontal bone when viewed laterally, a rugged nuchal area with a small nuchal hook, large projecting mastoid processes, and a rounded supraorbital margin. The mandible exhibited a projecting mental eminence and a broad chin that is U-shaped when viewed inferiorly. All of these traits are consistent with those of a male (see Buikstra and Ubelaker 1994; Burns 2013; France 1998; Krogman 1962). We also collected osteometric data from the cranium and the mandible. Although the right temporal and sphenoid bones exhibited slight postmortem damage and the right zygomatic arch was broken, all other standard metric data (see Buikstra and Ubelaker 1994) were gathered (Table 2). The data were processed through Fordisc 3®, an interactive discriminant function program, and assessed according to Walker's (2008) sex estimation regression equation. Both of these osteometric assessment methods support our anthroposcopic assessment.

Assessment of Age at Death

Evaluation of the degree of fusion of ectocranial sutures is useful for estimating the age of the decedent at the time of death (Meindl and Lovejoy 1985). Although cranial sutures are not as

https://doi.org/10.7183/2326-3768.1.2.91 Published online by Cambridge University Press

TABLE 1. Regional Cultural Chronology of the Cimarron District.

Phase	Dates
Jicarilla phase	A.D. 1750–1900
Cojo phase	A.D. 1550–1750
Regional abandonment?	A.D. 1300–1550
Cimarron phase	A.D. 1200–1300
Poñil phase	A.D. 1100-1250
Plateau phase	A.D. 300–900
Archaic	? – A.D. 300
Paleoindian	Although likely, no documented occupation

reliable for age determination as other bones of the skeleton, in this instance the cranium is the only skeletal material available for age estimation. Cranial sutures were graded at 17 different points and scored on a scale of 0–3, with 0 being completely open and 3 being fused and obliterated (see Mann et al. 1987; Meindl and Lovejoy 1985). Composite scores were calculated (Table 3) and an age range was determined. We observed the following: the anterior median palatine suture exhibited partial fusion. Significant fusion was exhibited on the mid-lambdoid, lambda, anterior-sagittal, mid-coronal, and transverse palatine. The following sutures exhibited obliterations: obelion, incisive, and posterior median palatine. Data were collected on bregma (open), pterion (partial fusion), sphenofrontal (partial fusion), inferior sphenotemporal (open), and superior sphenotemporal (partial fusion). The composite score of the lateral-anterior sutures was five, which indicates an age range of 27–51, with a mean age of 40. The composite score of the vault sutures was nine, which indicates an age range of 28–44, with a mean of 38. We also evaluated cranial suture closures using ADBOU©, a program that uses transition analysis to help assess age at death. ADBOU© age estimates for the cranium range from 21.4 to 41.2.

Dental eruption and wear also serve as indicators of age (White and Folkens 2005). The decedent's dentition includes all four third molars, and all the teeth show extreme attrition with much dentin exposure. The full eruption of all four third molars is consistent with an adult over the age of 25 (Suma et al. 2011; Tuteja et al. 2012). There was severe tooth wear, indicating either prolonged use, consumption of sediments in the diet, or some combination of the two. Tooth wear, especially in the American Southwest, is not a reliable age indicator due to the use of stone manos and metates in food preparation. Preparing food in this way can accelerate tooth wear (see Larsen 1995). Overall, the data support our age assessment; the decedent was possibly around 40 years of age at the time of his death.

Assessment of Ancestry

Ancestry of the skull was also assessed using anthroposcopic and osteometric methods. Although the common notion of race is discounted in the field of anthropology (Lieberman et al. 1989) and the continued use of racial categories is problematic for biological and forensic anthropologists (see Sauer 1992), skeletal remains often exhibit morphological traits suggestive of ancestral geographic origins (Ousley et al. 2009; Sauer and Wankmiller

TABLE 2. Cranial Metric Data Gathered Pursuant to Buikstra and Ubelaker (1994).

Cranial Metrics of the UU Bar Skull (mm)	
Maximum length (glabella to opisthocranion)	160
Maximum breadth (euryon to euryon)	144
Maximum width (bizygomatic diameter)	No data (damaged)
Maxillo-alveolar breadth (ectomolare to ectomolare)	68.5
Basion to bregma height	141.5
Cranial base length (basion to nasion)	102.5
Basion-prosthion length	97.5
Nasion to alveolar border	90.2
Mastoid length (Frankfort plane)	33.9
Nasal height (nasion to nasal spine)	55.1
Nasal breadth (alare to alare)	27.1
Upper facial height (nasion to prosthion)	75.4
Maxillo-alveolar length (prosthion to alveolon)	53.1
Biauricular breadth (auriculare to auriculare)	123.3
Minimum frontal breadth (frontotemporale to frontotemporale)	97.5
Upper facial breadth (frontomalare temporale to frontomalare to temporale)	105.6
Orbital breadth (dacryon to ectoconchion)	42.7
Orbital height (superior to inferior orbital margin)	34.4
Biorbital breadth (ectoconchion to ectoconchion)	96.0
Interorbital breadth (dacryon to dacryon)	15.7
Frontal chord (nasion to bregma)	108.4
Parietal chord (bregma to lambda)	95
Occipital chord (lambda to opisthion)	103.7
Foramen magnum length (basion to opisthion)	35
Foramen magnum breadth (lateral margin to lateral margin)	27.4
Chin height (infradentale to gnathion)	35
Height of mandibular body (alveolar process to inferior border)	32
Breadth of mandibular body	14
Bigonial breadth (gonion to gonion)	89.2
Bicondylar breadth (condylion to condylion)	125.1
Minimum ramus breadth	32.9
Maximum ramus breadth	44.1
Maximum ramus height	63.2

https://doi.org/10.7183/2326-3768.1.2.91 Published online by Cambridge University Press

TABLE 3. Cranial Suture Closure Scores (see Mann et al. 1987; Meindl and Lovejoy 1985).

Midlambdoid	2
Lambda	2
Obelion	3
Anterior-sagittal	2
Bregma	0
Midcoronal	2
Pterion	1 (skull damage may affect rating)
Sphenofrontal	1 (skull damage may affect rating)
Inferior sphenotemporal	0 (skull damage may affect rating)
Superior sphenotemporal	1 (skull damage may affect rating)
Incisive Suture	3
Anterior Median Palatine	1
Posterior Median Palatine	3

2009; SWGANTH 2013), which is of considerable relevance in terms of repatriation efforts. Accordingly, in bioarchaeology and forensic anthropology, humans are categorized into ancestral groups that often exhibit morphological distinctions that aid in the identification of skeletonized remains: African, Asian/Native American, and Caucasian. We observed that the UU Bar cranium is quite rounded. The face is wide and exhibits slightly projecting zygomatic bones. The eye orbits are mostly rounded (albeit with some angularity) and the lower eye borders are slightly projecting. The nose has a low and ridged root, exhibits a low bridge of intermediate width, and has a flat and sharp lower border. The cranial sutures are complex and the postbregma is flat. The mandible is large, with a vertical ramus, and the chin is rounded. Features of dentition, specifically shovel-shaped incisors, are a common indicator of Native American ancestry (Scott and Turner 1988). Although the incisors are considerably worn, they do bear some evidence of shoveling. Anthroposcopically, the decedent's traits are consistent with those of a Native American. Osteometric data from the cranium and mandible (see Table 2) were also evaluated with Fordisc 3® and Osteoware©, both of which support our anthroposcopic assessment. Accordingly, we conclude, based upon these assessments, together with the geographic region in which the remains were found, that the remains are those of an adult male of Native American ancestry, approximately 40 years of age at the time of death, who died of cause or causes unknown.

Optically Stimulated Luminescence (OSL)

Because we agreed to avoid destructive methods in our analysis of the remains, we were unable to submit a sample for radiocarbon dating. Noting that the cranium had become filled with sediments in the years following interment, we opted to use OSL to place the remains in a cultural-chronological context. Although the remains would be older than the age of the sediments that filled the cranium during the years following death and decomposition, the age of sediment deposition would provide a time frame for the initial burial of the remains. This in turn would provide at least some guidance regarding repatriation efforts. The specific advantage of OSL is that it provides a non-destructive, numerical dating method for determining the age range of human remains when either the burial location is known or, as in this case, the remains themselves happen to allow for preservation of sediments.

OSL is a method for determining the age of the last deposition of quartz and feldspar-bearing sediments if the sediments have been exposed to sufficient light during the erosional path or anthropogenic event. These naturally occurring minerals act as dosimeters when exposed to the emissions of radioactive isotopes, including uranium (U), thorium (Th), and potassium (K). The amount of energy absorbed via electron excitation to local "traps" within the mineral lattice is proportional to the "dose rate" and the time since the mineral was last "zeroed," either by exposure to sunlight or intense heat above 300°C. The stored energy is then released when exposed to either laboratory or natural events, and this measurement is known as the "equivalent" or "paleo dose," which is the amount of stored energy in terms of received dose (proportional to the amount of light). The paleo dose is determined in the lab by calibrating against radioactive laboratory sources, usually a beta source. This measurement, when combined with the measured dose rate (energy delivered/year), allows the time of deposition to be determined (Bishop et al. 2005; Duller 2008a; Rhodes 2011) and thus can be used as a chronometer. This procedure is referred to as luminescence geochronology, the goal of which is to establish the timing of the burial of mineral grains in sedimentary deposits.

Radiocarbon dating of bone from archaeological sites is common (e.g. Huckleberry et al. 2003), albeit sometimes problematic (Highman et al. 2006). However, more recently, OSL on quartz and IRSL on feldspars have been used with impressive results. Both quartz and feldspar (IRSL) were used to date sediments that contained 49 artifacts (no human remains) from the Buttermilk Creek Paleoindian site, all of which produced consistent ages (see Waters et al. 2011), and quartz OSL is being used to date the sediments at the Topper Site (see Waters et al. 2009), assuming the problem of bioturbation can be overcome. OSL has been used extensively in Europe, Australia, Africa, and Asia for dating artifacts, human remains, and other anthropogenic activities (Duller 2008a; Jacobs et al. 2008). In a particular case study from Australia that bears some similarity to this case, OSL was measured from sediment encased in a cavity of a kangaroo skull, and the result documented much older ages than expected (~ 40 ka) (Prideaux et al. 2010; Roberts et al. 2001). What is unique about the discovery in New Mexico is that, even though the original location of the burial is unknown and thus luminescence dating of the burial site itself cannot be conducted, OSL can be used to date the tightly compacted sediments fortuitously trapped in the cranium.

OSL Methodology and Sampling

In an artificially darkened environment, we extracted core samples of the impacted sediments through the foramen magnum, the large opening at the base of the skull where it articulates with the spinal column (Figure 3). A hand drill was used to bore

https://doi.org/10.7183/2326-3768.1.2.91 Published online by Cambridge University Press

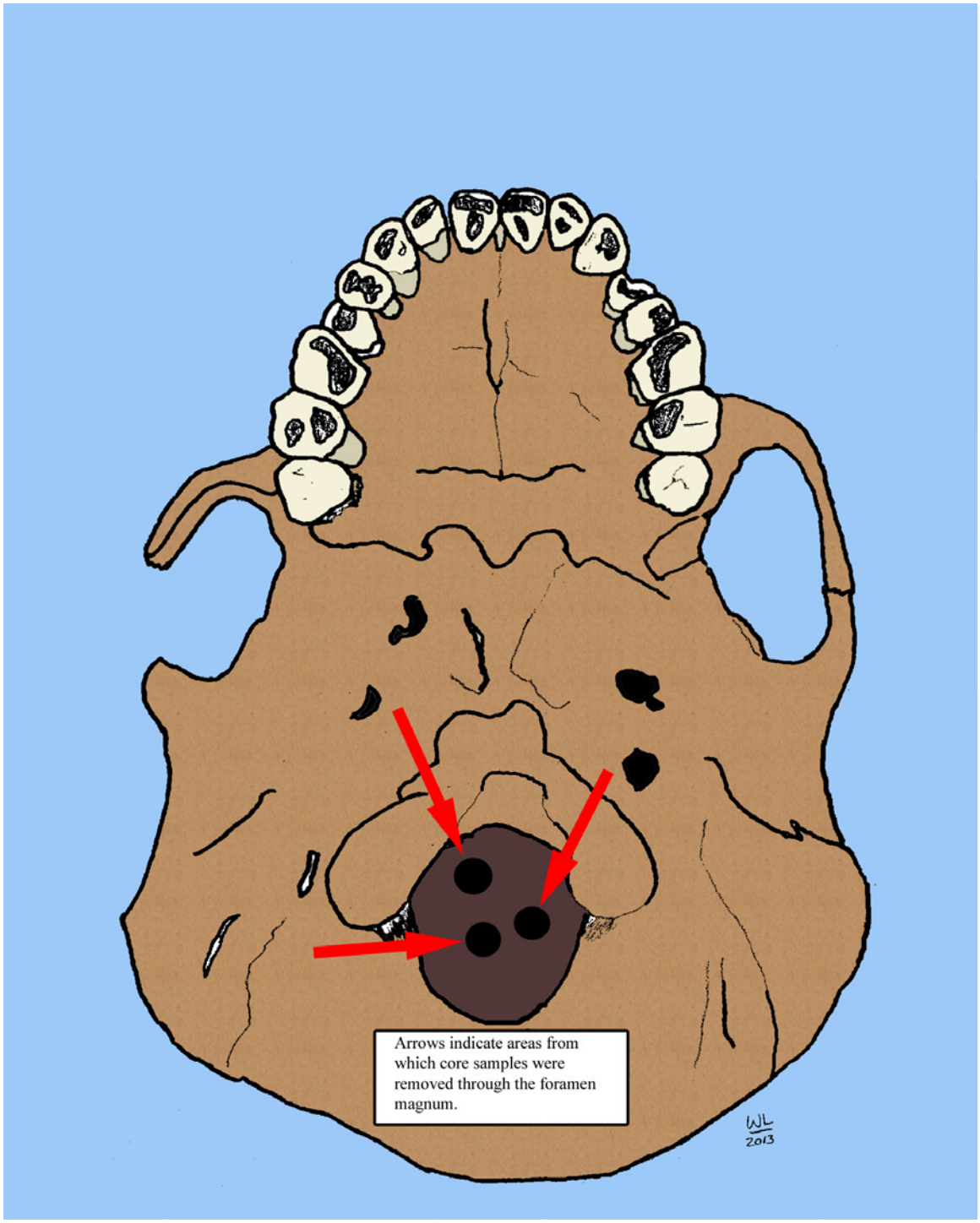


FIGURE 3. Sketch of cranium depicting areas where sediment cores were removed through the foramen magnum (arrows). Illustration by Warren Lail.

two holes ~ 7–8 mm in diameter to a depth of ~10 cm. The sediments from the bottom ~ 5 cm of the boreholes were obtained without allowing the drill to touch the bone, thereby causing no damage. Two 20 g sediment samples were extracted. However, in order to obtain enough quartz grains for luminescence measurements, all of the sediment core materials below ~ 2.5–3 cm were combined into a single sample.

The source of the sediments encased in the skull is believed to be the Sangré de Cristo Formation "red beds," which are composed of coarse- and fine-grained mixed clastics, predominantly of dark-red and reddish-brown sandstone and conglomerate exposed in places along Cimarroncito Creek (Robinson et al. 1964). The sediments exhibit a red hue (dry 2.5 YR 5/2, weak red) likely due to staining by iron hydroxide ($Fe(OH)_2$) (see Robinson

https://doi.org/10.7183/2326-3768.1.2.91 Published online by Cambridge University Press

et al. 1964). Additionally, the skull itself exhibits a similar red hue (5YR 5/2, reddish gray) probably caused by exposure to the mineral-laden fluvial sediments. The texture of the soil encased in the cranium was assessed and estimated by hand. All samples appear to be clay loam (CL) (see Schoeneberger et al. 2012).

Normally when conducting OSL analyses, modern soil samples are collected near the burial site and either horizontal or vertical subsampling would also take place (from 0 to 5 cm in large incremental scales). These tests help determine whether the modern sample carries essentially a "zero dose" (0.1-0.3 Gy), whether bioturbation is a common problem at the site, and whether there is a possibility of slow sedimentation rates (in our case, whether the cranium would have filled slowly or quickly). We were unable to sample soils from the extraction site because, even after considerable pedestrian survey, the location from which the remains were originally recovered was not found. Moreover, the terraces and geologic exposures vary considerably along Cimarroncito Creek (see Robinson et al. 1964) and, therefore, random sediment sampling would have been of little value.

Dosimetry or Dose Rate (D_R)

Water content of the sediment sample was measured at a very dry 0 percent in the lab, with the understanding that the sediment more than likely dried out while stored at the museum. Accordingly, we do not know the original field value. We were thus required to proceed with some reasonable assumptions. We know that in the study area the spring and summer seasons yield about three quarters of the annual moisture, with most precipitation occurring during the summer monsoon (Tuan et al. 1973(18):30–33). The remainder comes from localized winter snow and from the snowpack that accumulates higher in the mountains (Lail 2008). Historically, a range of 22.8 cm (9 in) to 63.5 cm (25 in) total precipitation falls annually in the Cimarron District (see Lail 2008). The dose rate was calculated as 6 percent moisture for a best estimate of the water budget of the sediment year-round, i.e., pore spaces would have been filled with water 6 percent of the time. This translates to an annual average of 5 to 7 percent water in the sediment each year. This moisture value may be too low if the water table near the creek was high enough to reside at the level of the skeletal remains, but the generally excellent preservation of the skull makes it improbable that the water content of the soil was much higher than 10 percent or remained for a long interval at the maximum soil moisture of 25 percent. Maximum soil moisture was measured in the lab by performing centrifuge tests of the sediments removed from the cranium. This was accomplished by immersing the sediments in water and then centrifuging them at high speed. The water was then decanted and the wetted sediments weighed to obtain an approximation of the full saturation potential. The generally fine-grained sediments encased within the skull may also have affected moisture measurements, but because the sediments are all generally sourced from the same geology and environment, no additional parameters were considered.

The dose rate (D_R) was obtained using elemental concentrations (K, U, Th, and Rb) as determined from Inductively-Coupled Plasma Mass Spectrometry (ICP-MS) following the procedures described at http://minerals.cr.usgs.gov/icpms/intro.html. Alpha and beta contributions to the D_R were corrected for grain-size attenuation (Aitken 1985). Cosmic-ray D_R data were estimated for each sample as a function of depth, elevation above sea level, and geomagnetic latitude (Prescott and Hutton 1988, 1994). The depth was taken from notes in the museum archives showing the height above the creek bank and below the terrace top where the remains were found.

ICP-MS Preparation and Analyses

Generally, solid samples must be converted into an aqueous form through the use of an appropriate sample digestion technique before being analyzed on the ICP-MS. Measured elemental concentrations, associated D_R, and cosmic ray contributions are presented in Table 4. These count rates are accurate for estimating and calculating D_R provided there is no significant disequilibrium of the uranium-thorium decay chain. Radioactive disequilibrium is assessed by looking at the differences in the isotopes measured for uranium and thorium (for example, ICP-MS measures ^{39}K, ^{238}U, and ^{232}Th, while high purity germanium detector gamma spectrometry measures ^{40}K, equivalent inferences of peaks at ^{226}Ra, ^{214}Bi, ^{214}Pb for U, while Th is also measured by equivalent inferences of peaks at ^{228}Ac and ^{212}Pb). However, it should be noted that thorium is usually in equilibrium in sediment samples. Based upon our elemental concentrations for U:Th of 1:3, we assume no disequilibrium.

The bulk sample was dried, homogenized by crushing to a fine powder in a Shatterbox™ pulverizer, and then placed in a lab digestion cation-exchange resin column. Sample decomposition using this multi-acid digestion technique is well suited to dissolve certain rock types, soils, and sediments. This method uses a combination of nitric, hydrochloric, hydrofluoric, and perchloric acids. Errors on the measurements were calculated by looking at the calibration standards used during the measurement cycle.

Equivalent dose determination (D_E)

We used film canisters as storage for the drilled cores during sampling, and all operations took place under artificially darkened conditions. The exposed surface of the sediment was separated from the rest of the core and used for the dosimetry (dose rate) analyses. The lower sections of the cores were used for the D_E analyses on the expectation that they would have remained darkest during exhumation and any subsequent transportation of the skull.

The entire volume of the extracted sediment, after removing 2.5–3 cm of the possibly light-contaminated material from core surface, was leached in 4N HCl (10 percent HCl) for 24 hours to dissolve any post-depositional carbonate coatings, 35 percent H_2O_2 for 24 hours to dissolve the organic and soil carbonates, and 10 percent HF for 20 minutes to dissolve surface impurities such as iron oxides from the quartz grains. The coarser grain (90–250 µm or 170–80 mesh) quartz fractions were separated from the feldspars using heavy liquids (lithium sodium polytungstate) (ρ = 2.58 gcm^{-3}) and heavy minerals using a Franz magnetic separator. The sink from density 2.58 was subjected to a 50 percent solution of HF acid for 40 minutes while in an ultrasonic bath. After pouring off the HF solution, we put the sample in 6N HCl for five minutes (still in the ultrasonic bath) and finally re-sieved to winnow out broken feldspar grains.

Steel target discs were dabbed with a small circle of silica spray, known as a 1mm mask, and a single grain-thick layer of these refined quartz grains was dispersed onto the discs. Approxi-

https://doi.org/10.7183/2326-3768.1.2.91 Published online by Cambridge University Press

TABLE 4. Summary Quartz OSL Data and Ages from UU Bar Ranch Skull.

Sample information	% Water content[a]	K (%)[b]	U (ppm)[b]	Th (ppm)[c]	Cosmic dosec (Gy/ka)	Total Dose Rate (Gy/ka)	Equivalent Dose (Gy)	n[d]	Age (yrs)[e]
PR-1 (2 Gy)	0 (25)	1.94 ± .07	5.47 ± .22	15.8 ± .52	.31 ± .03	4.57 ± .11	2.41 ± .15	15 (41)	556 ± 35.9
PR-1 (4 Gy)	0 (25)	1.94 ± .07	5.47 ± .22	15.8 ± .52	.31 ± .03	4.57 ± .11	4.72 ± .21	16 (41)	1,091 ± 54.5

a. Field moisture, with figures in parentheses indicating the complete sample saturation %. Ages calculated using approximately 25% of saturation values.

b. Analyses obtained using ICP-MS.

c. Cosmic doses and attenuation with depth were calculated using the methods of Prescott and Hutton (1994). See text for details.

d. Number of replicated equivalent dose (De) estimates used to calculate the equivalent dose. Figures in parentheses indicate total number of measurements included in calculating the represented equivalent dose and age using the minimum age model (MAM). All aliquots passed methodology tests.

e. Dose rate and age for fine-grained 250-90 microns quartz sand. Linear fit used on equivalent dose, errors to one sigma.

mately 50 to 150 grains were used for each disc. The discs were then loaded onto a carousel for luminescence analyses. About 40 aliquots were measured to ensure the most reliable statistical trends (see Rodnight 2008). All the aliquots returned a signal and, based upon the OSL characteristics (recycling ratios, test dose response, and recuperation ratios), all aliquots produced acceptable data (Figure 4).

Blue-light OSL was conducted on fine sand-size quartz separates using single aliquot regeneration (SAR) protocols (Table 5). Light stimulation of the quartz was achieved using a RISØ TL-DA-15™ reader with an array of blue-light-emitting diodes (LEDs centered at 470 nm or15 MW/cm^2). Detection optics included Hoya 2×U340 and Schott BG-39 filters coupled to an EMI 9635 QA Photomultiplier tube. β radiation was applied using a 25 mCi ^{90}Sr/^{90}Y in-built source.

The main SAR parameters included use of continuous-wave OSL (CW-OSL) at the 40-second blue-diode stimulation step recommended by Murray and Wintle (2003) with the sample measured for OSL while at 125˚C, and subsequently at the same preheat temperature of 200˚C using continuous-wave OSL (CW-OSL). The first 0.8 seconds of this stimulation generally releases the preferred component of SAR dating known as the "fast component" (Murray and Wintle 2000; Wintle and Murray 2006). SAR was used because a dating precision of ~ 10 percent (sometimes better) can be attained routinely with multigrain SAR quartz methods (Murray and Olley 2002) when applied to aeolian sand. With SAR, each aliquot yields a distinct D_E value and thus a distinct age estimate.

The choice of preheating temperature for each sample was based upon preliminary dose recovery and preheat plateau test experience with samples of similar properties and lithology. All sample aliquots were run at 200°C for ten seconds, depending on the initial estimate of equivalent doses.

Several quality-control criteria were employed to reject OSL signals and resultant SAR D_E values. Data rejection criteria were similar to those in common practice (Wintle and Murray 2006) and D_E growth curve data were fit to a linear trend. The growth of the luminescence with increasing dose was represented well by a simple linear function and illustrates the generally reliable behavior of the quartz samples for the SAR protocol (Figure 4b). We accepted data having "recycle" ratios within 10 percent of 1.0 and "recuperation" ratios (Aitken 1998) within 2 percent of zero when recuperation was > 20 percent of the normalized "natural" signal (Lx/Tx ratio), and test-dose-signal errors were < 10 percent. We forced dose-response curves through the origin. Dose recovery and preheat plateau tests were performed to ensure that the sediments were responsive to optical techniques and that the proper preheat temperatures were used in producing the equivalent dose (D_E) values. The preheat tests showed that preheat temperatures from 160°C to 260°C would be acceptable, but our experience with young samples led us to keep the preheat temperature at 200°C in all measurements.

ANALYSIS

In many quartz-pure samples, three main components of OSL have been observed and are informally called the "fast," "medium," and "slow" components (Bailey et al. 1997). The fast component of OSL is generally required for accurate analysis and reliable age determination, unless one wishes to engage in time-consuming efforts to de-couple the growth curve components. The sharp decay of the initial part of the signal in these samples suggests dominance by the fast component and therefore did not require additional efforts to separate the components. Every aliquot returned a signal. Because the dose rate was high (around 4 Gy/ka), a signal would have developed rather quickly after burial; in this case, that was an unexpected bonus. The data therefore did not suffer from signals that were barely above background or otherwise insensitive to stimulation and measurement.

The dispersion of the equivalent doses (48.7 percent) obtained in the sample shows skewness, which is distortion or bias or not having equal properties above and below the mean (Figure 5). Skewness is normal for samples that have a shallow fluvial or alluvial origin or many generations of depositional cycles with extensive bioturbation within the sediment (Duller 2008a). There are two models for dealing with high skewness, both of which strive to retain the most appropriate measure of equivalent

https://doi.org/10.7183/2326-3768.1.2.91 Published online by Cambridge University Press

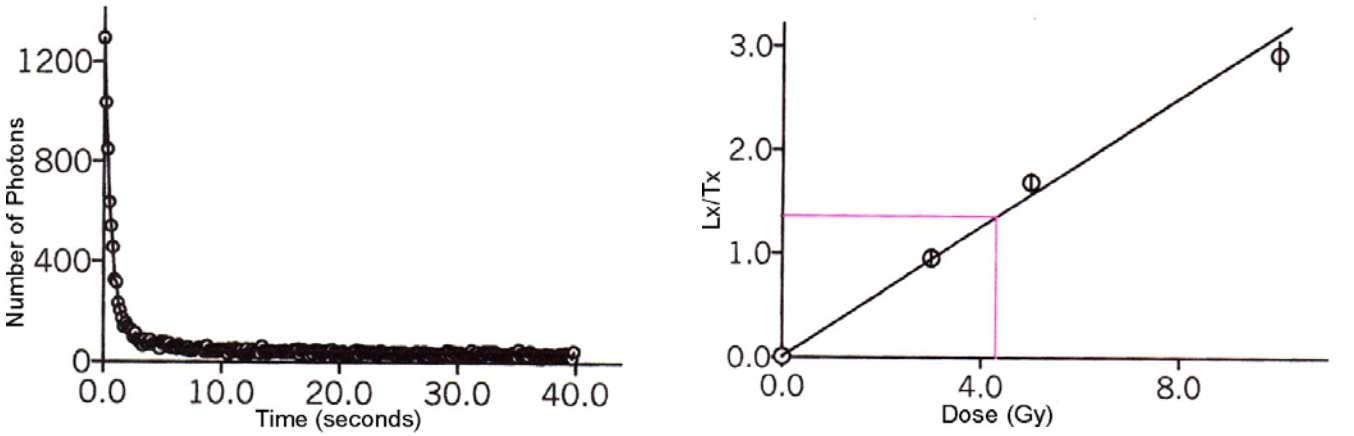


FIGURE 4. (a) An OSL decay curve for PR-1 showing the quartz signal as measured with blue-light wavelength emitting diodes. The x-axis is time of measurement in seconds (s) and the y-axis is photon counts/second over the course of the 40-second measurement period (here a little over 1200 cts at the start of the LED's stimulation). A sharp decay is seen after 1 to 2 seconds of stimulation, indicating access from a fast component of OSL. The OSL equivalent dose data are taken from the initial part of the first .5 sec. and the background adjustment is taken from the last second of the 40-second measurement. (b) PR-1 growth curve, with the natural (red lines) plotted on the Lx/Tx axis below 1.0. The x-axis is the equivalent dose measured in Grays (shown circles are obtained at 3 Gy, 5 Gy, 10 Gy). The natural hits the linear line at about 4 Gy for this particular aliquot. The bleach (zero) is shown at the junction of the axes. The y-axis shows the luminescence response over the test dose response (Lx/Tx or unitless normalized OSL sensitivity measurements).

dose. The choice is between a measure of central tendency for samples without large partial bleaching or bioturbation problems and a minimum age model that tries to capture the younger part of the distribution. The central tendency model is preferred when both skewness (balance) and overdispersion (scatter) are deemed low, whereas the minimum age model is preferred when the samples show skewness with obvious partial bleaching or bioturbation (Galbraith 2005; Galbraith et al. 1999). Accordingly, we chose to use the minimum age model, but we considered two populations of equivalent dosage (Table 4; see Arnold et al. 2007 for further details regarding the minimum age model).

DISCUSSION

OSL age calculations are normally based directly on both the mean and standard error of the D_E data as well as propagated age uncertainty. These calculations take geological uncertainties into consideration, thus leading to a one-sigma error determination (68 percent confidence level) (Lepper et al. 2011). The accuracy of luminescence ages depends on a number of parameters, such as systematic errors, whereas precision depends largely on random errors. Systematic errors are controllable to some degree, but they are site-dependent (either field or lab) and involve measurement discrepancies. These include such factors as water content of the sediment over time, cosmic dose component (varying with elevation and depth over time), errors in the calibration of the gamma or beta sources used to irradiate the sample in the lab, or suitability of the sediment (or material) for use with the single-aliquot regeneration procedure (Duller 2007). Random errors, on the other hand, are uncontrolled factors that influence the result of measurement or the stochastic nature of the process. Examples include variation in the brightness of D_E in grains, assessing the sensitivity of the D_E signal, assumptions regarding the form of the dose response, errors in individual L/T ratios, or transforming the error in the L/T ratios to an error in D_E. This kind of error generally tends to swamp out the uncertainties arising from the systematic errors (Aitken 1976; Aitken and Alldred 1972; both summarized in Aitken 1985).

Because we obtained two sets of luminescence data, we had to determine which set was likely to be the most appropriate to use for an age calculation for the skull (see radial plot, Figure 5). One population is centered at 2.4 Gray (Gy) within a two-sigma band of possibility, and the second population is centered at 4.7 Gy, also within a two-sigma band. Four other aliquots (around 7 to 9 Gy) were removed from the age calculation because it is likely that these were largely a result of partially bleached grains. There was little to no overlap between the 2.4 Gy and 4.7 Gy populations. Our tests indicate that the quartz had the "fast" component of OSL, was sensitive to the blue-light stimulation, and returned bright signals (Figure 4). Although the quartz grains returned two D_E values, this is due to geological and not mineralogical factors. While there are other ways to explain dispersion or scatter in the D_E, we discount the idea that the D_E dispersion would have been generated from vertical or horizontal bioturbation within or around the skull based upon its excellent state of preservation and the general uniformity of sediment within the cranium. These features (intact teeth and articulated cranial bones) would not have survived extensive bioturbation. The possibility that there would be two different depositions that then got mixed inside the skull (i.e., the skull partially filled, then was buried and completely filled) also does not seem very likely. For there to be two different depositions, the skull would have had to lie on or close to the surface for some time and, again, it seems fairly implausible that the skull would have survived if that had been the case. By obtaining an age based only on the lowest D_E population that we measured, we have endeavored to provide our very best hedge against small biota

https://doi.org/10.7183/2326-3768.1.2.91 Published online by Cambridge University Press

TABLE 5. Luminescence Protocols Followed in Preparation and Analysis of Samples for Quartz OSL.

Measurement parameters:	
Machine:	Automated Risø TL/luminescence-DA-15
Mineral; grain size:	Quartz: 250-90 µm
Stimulation source:	Blue LED diodes, emission centered on 470 nm
Power delivered to aliquot:	14 mW/cm^2 (90% power)
Duration of stimulation:	40 seconds
Final signal level:	3% of initial
Photomultiplier:	Thorn-EMI 9235Q
Aliquot temperature:	125°C
Detection filters:	Two Hoya U340 filters
Normalization:	None
Preheat:	200°C (samples < 5 ka) for 10 secs
Delay before measurement:	120 sec
Equivalent dose evaluation:	Single aliquot regeneration (Murray and Wintle 2000, 2003)
Background evaluation:	Black body counts < 30 ct/sec, BG counts <39 ct/sec
Alpha effectiveness:	n/a
Dose-rate evaluation:	ICP-MS elemental concentrations
Dose rate range:	4.46–4.68 Gy/ka (Grays per thousand years)
Water content:	25% of full saturation potential (this equates to 6% water moisture)
Cosmic-ray contribution:	7% of total dose rate, independent of sampling site

processes that may have mixed the sediment. Small biota is defined as worms or ants that disturbed sediment layers. Rink et al. (2013) found that ants commonly move soil upwards and that age overestimation is the major expected affect.

Depending on the cultural burial rites of the associated tribe, we arrive at one of two determinations. If the bodies were buried in the terrace, we suggest that the dimmest signals must have been those grains that reset during the actual burial event. This burial would have exposed some grains to sunlight but left the majority in various stages of bleached disarray. As the body decayed and cavities opened, the grave and terrace grains would have mixed as they filled the cranium. Alternatively, if the bodies were simply laid upon the site (or were already in place) and had decomposed sufficiently to provide pockets for the collection of sediments during a minor flood or collapse of a channel bank soon after the bodies were in situ, then the skull would have filled slowly with grains as the cavities opened. This would suggest that the infilling occurred over a considerable period of time. On the other hand, the infilling could have taken place quickly if the particular event was due to a substantial flood. In either case, the simplest explanation is that the grains show a variety of responses to partial bleaching, and those grains that were most likely fully bleached during burial will have the smallest (youngest) D_E signal.

Our research shows that the age associated with the smallest D_E grain population (at 2.4 Gy) is 555 years (A.D. 1455; ± 40 years, rounded figures). The age from the next largest equivalent dose grain population (at 4.7 Gy) is 1,090 years (A.D. 920; ± 55 years, rounded). Many methods have been advanced in the OSL literature that strongly support the approach of using only the smallest population of equivalent dose, because this best represents those grains that were fully bleached at time of deposition (Duller 2007; Rittenour 2008). These same studies (summarized in Rittenour 2008) have shown that most sediment is dateable by single aliquot techniques in spite of partial bleaching problems and return ages that have later correlated to other dating methods (Feathers et al. 2006; Murray et al. 2012). Accordingly, we estimate the age of the skull to be between 515 and 595 years old and thus not buried before A.D. 1415 or after A.D. 1495 (Table 4, values rounded for discussion).

CONCLUSIONS

Our objective was to study and repatriate the culturally unidentifiable prehistoric Native American remains found along Cimarroncito Creek without using any destructive analytic methods. Accordingly, we chose Optically Stimulated Luminescence (OSL), which provides a non-destructive, numerical dating method that can be used to date human remains when the burial location is known or, in the case of the UU Bar skull, compacted sediments have filled the cranial cavity. Core samples of sediments were removed through the foramen magnum and measured using only OSL, and while the results are not as precise as those obtained from radiocarbon dating, we were able to place the remains within a regional chronological context without causing damage to the skull.

The Cimarron District was likely largely uninhabited during the period A.D. 1300 to 1550 (see Table 1). However, given that our

https://doi.org/10.7183/2326-3768.1.2.91 Published online by Cambridge University Press

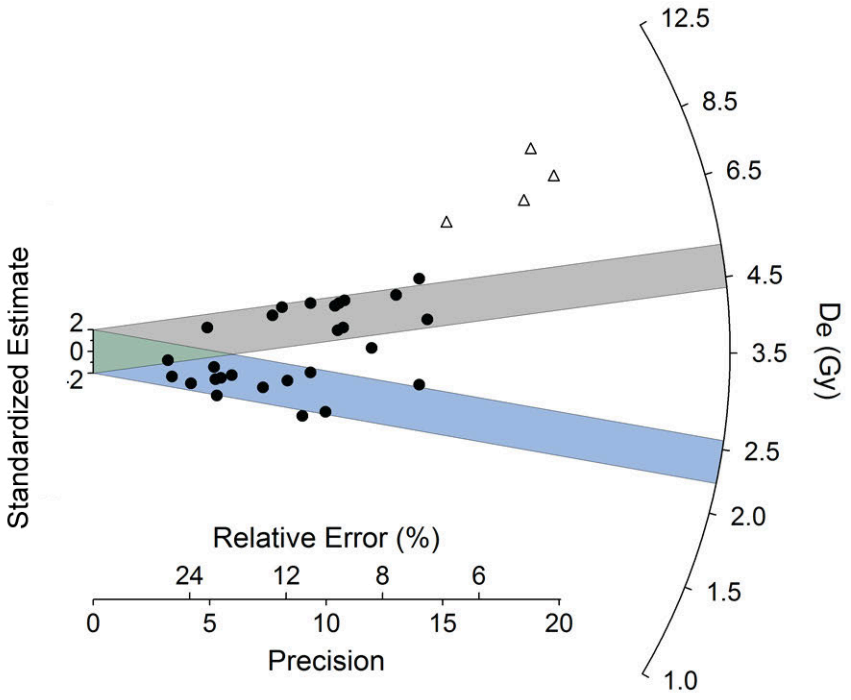


FIGURE 5. Radial plot graphical analyses for PR-1 that allows visualization of equivalent dose distributions, where focus is drawn to the best-known results (Wallinga 2002). The number of aliquots = 35 (41) is shown. Note that there are two populations of grains, one in green (centered at 2.4 Gy) and one in yellow (centered at 4.7 Gy). There are four aliquots showing partial bleaching (7.4, 7.6, 7.9, and 9.4 Gy) that plot completely out of the two-sigma populations and therefore are not included in the averaged equivalent doses. The large equivalent doses related to partial bleaching (see appendix; 11-29 Gy) were not included in this plot.

data show that the skull was possibly buried shortly before A.D. 1415 but no later than A.D. 1495, we believe that the remains are possibly from individuals of the Ute Mouache Band, who once traversed the southern Rockies and western margins of the Great Plains in northern New Mexico beginning roughly around A.D. 1400 (see Simmons 2000) and continuing into the late 1800s (Keleher 1964). Following the guidelines of the 2010 Final Rule, we are now in the process of notifying the Southern Ute Indian Tribe, Ignacio, Colorado, to begin the consultation for the proper repatriation of the remains.

RECOMMENDATIONS FOR FUTURE RESEARCH

We recommend that when archaeologists recover skeletal remains they not remove the sediments from the cranium in routine laboratory cleaning, but instead leave the sediments intact to facilitate this non-destructive dating method. Likewise, we recommend that sediments in ceramic vessels be treated similarly. If sediments are removed, then we recommend that the removal take place in a darkened lab and that the sediments be preserved in light-tight containers for future OSL testing. We also recommend that museums and other repositories of culturally unaffiliated human remains examine crania for impacted sediments that might be used for OSL dating, which may assist in repatriation efforts under the 2010 Final Rule.

Finally, we recommend that, when possible, modern soil samples should be collected from somewhere near the burial site and that horizontal or vertical subsampling take place (from 0 to 5 cm in a large incremental scale). These tests would answer questions about whether the modern sample carries essentially a "zero dose" (.1–.3 Gy), whether bioturbation is a common problem at the site, and whether there is a possibility of slow sedimentation rates. We also recognize that single-grain dating of the quartz sand-sized grains preferentially opens up a wider range of potential environments and new possibilities for understanding post-depositional grain movement (Rhodes 2011) because it improves reliability by assessing whether individual grains were in fact bleached at deposition, thus mitigating the possibility of measuring any prior trapped charge and providing increased accuracy (see Duller 2008b). In our case, however, we believe that the accuracy of our sampling technique is sufficient for the purpose intended: to provide a general time frame to aid in the repatriation of the remains.

Acknowledgments

The authors are grateful for NSF support via DMR grant 0934212 (PREM). We also wish to acknowledge the support of the Department of Social and Behavioral Sciences, the Department of Chemistry and Biology, and the University Research Laboratory of Anthropology at New Mexico Highlands University. We also acknowledge and thank the USGS Luminescence Dating Lab, Denver, Colorado, the Philmont Museum, the Philmont

https://doi.org/10.7183/2326-3768.1.2.91 Published online by Cambridge University Press

Scout Ranch, and Dr. David Kirkpatrick for making this research possible. A special thanks goes to Aaron Roth, M.A., who helped conduct a de novo analysis of the cranial features. We thank the National Science Foundation for a grant of $384,926 to fund the acquisition of an Automated TL/OSL Luminescence Reader, Gamma Spectrometer, and Portable Field Gamma Spectrometer for the Dating of Sedimentary and Archaeological Materials at New Mexico Highlands University (grant author and principal investigator, David Sammeth, Ph.D.). Finally, we thank the reviewers and the editor for comments and suggestions that substantially improved this paper.

Data Availability Statement

All of the data referenced in this article are included herein. The skeletal remains are housed in the curatorial facilities at the Research Laboratory of Anthropology at New Mexico Highlands University, Las Vegas, New Mexico. Contact Warren Lail, JD, Ph.D., Department of Social and Behavioral Sciences, Box 9000, Las Vegas, NM 87701 for information or access while the remains await repatriation. For information relating to OSL, contact Shannon Mahan, Director, USGS Luminescence Dating Lab, Box 25046, MS 974, Building 15, Denver Federal Center, Denver, CO 80225.

References Cited

25 U.S.C. 3001 et seq.

1990 Native American Graves and Repatriation Act.

43 CFR 10

2010 Native American Graves Protection and Repatriation Act Regulations—Disposition of Culturally Unidentifiable Human Remains; Final Rule.

Aitken, M. J.

1985 *Thermoluminescence Dating*. Academic Press, London.

1998 *An Introduction to Optical Dating*. Oxford, Oxford University Press.

Aitken, M. J., and J.C. Alldred

1972 The Assessment of Error Limits in Thermoluminescent Dating. *Archaeometry* 14(2):257–267.

Arnold, L., R. Bailey, and G. Tucker

2007 Statistical Treatment of Fluvial Dose Distributions from Southern Colorado Arroyo Deposits. *Quaternary Geochronology* 2:162–167.

Bailey, R., B. Smith and E. Rhodes

1997 Partial Bleaching and the Decay Form Characteristics of Quartz OSL. *Radiation Measurements* 27:123–136.

Berg, Gregory E.

2008 Biological Affinity and Sex Determination Using Morphometric and Anthroposcopic Variables from the Human Mandible. Ph.D. dissertation, Department of Anthropology, University of Tennessee.

Bishop, P., D. Sanderson, J. Hansom, and N. Chaimanee

2005 Age-Dating of Tsunami Deposits: Lessons from the 26 December 2004 Tsunami in Thailand. *The Geographical Journal* 171(4):379–384.

Buikstra, J. E., and Ubelaker, D. H.

1994 Standards for Data Collection from Human Skeletal Remains. Fayetteville, AR. Arkansas Archaeological Survey Research Series 44.

Burns, Karen R.

2013 *Forensic Anthropology Training Manual*. 3rd ed. Pearson, Boston.

Duller, G.A.T.

2007 Assessing the Error on Equivalent Dose Estimates Derived from Single Aliquot Regenerative Dose Measurements. *Ancient TL* 25:15–24.

2008a *Luminescence Dating: Guidelines on Using Luminescence Dating in Archaeology*. English Heritage, Swindon.

2008b Single-grain Optical Dating of Quaternary Sediments: Why Aliquot Size Matters in Luminescence Dating. *Boreas* 37:589-612.

Feathers, James K., Vance Holliday, and David Meltzer.

2006 OSL Dating of Southern High Plains Archaeological Sites. *Journal of Archaeological Science* 33:1651–1665.

France, D.

1998 Observational and Metric Analysis of Sex in the Skeleton. In *Forensic Osteology: Advances in the Identification of Human Remains*, edited by K. J. Reichs. 2nd ed. Charles C. Thomas, Springfield, Illinois.

Galbraith, R.

2005 *Statistics for Fission Track Analysis*. Chapman and Hall/CRC, Boca Raton.

Galbraith, R., R. Roberts, G. Laslett, A. Yoshide, and J. Olley.

1999 Optical Dating of Single and Multiple Grains of Quartz from Jinmium Rock Shelter, Northern Australia, Pt. I: Experimental Design and Statistical Models. *Archaeometry* 41:339–364.

Highman, T.F.G., R.M. Jacobi, and C. Bronk Ramsey

2006 AMS Radiocarbon Dating of Ancient Bone Using Ultrafiltration. *Radiocarbon* 48(2):179–195.

Huckleberry, Gary, Julie Stein and Paul Goldberg.

2003 Determining the Provenience of Kennewick Man Skeletal Remains through Sedimentological Analyses. *Journal of Archaeological Science* 30:651–665.

Jacobs, Z., R. Roberts, R. Galbraith, H. Deacon, R. Grün, A. Mackay, P. Mitchell, R. Vogelsang, and L. Wadley.

2008 Ages for the Middle Stone Age of Southern Africa: Implications for Human Behavior and Dispersal. *Science* 322:733.

Keleher, William A.

1964 *The Maxwell Land Grant*. University of New Mexico Press, Albuquerque.

Krogman, M.

1962 *The Human Skeleton in Forensic Medicine*. Charles C. Thomas, Springfield, Illinois.

Lail, Warren K.

2008 Behavioral Regions Analysis of the Poñil Canyon, Colfax County, New Mexico. Ph.D. dissertation, Department of Anthropology, University of Oklahoma, Norman.

Larsen, Clark S.

1995 Biological Changes in Human Populations with Agriculture. *Annual Review of Anthropology* 24:185–213.

Lepper, K., K. Gorz, T. Fisher, and T. Lowell.

2011 Age Determinations for Glacial Lake Agassiz Shorelines West of Fargo, North Dakota, USA. *Canadian Journal of Earth Sciences* 48:1199–1207.

Lieberman, Leonard, Blaine W. Stevenson, and Larry T. Reynolds

1989 Race and Anthropology: A Core Concept without Consensus. *Anthropology and Education Quarterly* 20(2):67–73

Mann, R., S. Symes, and W. Bass

1987 Maxillary Suture Obliteration: Aging the Human Skeleton Based on Intact of Fragmentary Maxilla. *Journal of Forensic Sciences* 32:148–157.

Meindl, Richard S. and C. Owen Lovejoy

1985 Ectocranial Suture Closure: A Revised method for the Determination of Skeletal Age at Death Based on the Lateral-Anterior Sutures. *American Journal of Physical Anthropology* 68:29–45.

Murray, A., and A. Wintle

2000 Luminescence Dating of Quartz Using An Imroved Single-Aliquot Regenerative-Dose Protocol. *Radiation Measurements*. 32(1):57–73.

2003 The Single Aliquot Regenerative Dose Protocol: Potential for Improvements in Reliability. *Radiation Measurements* 37:377–381.

Murray, A., and J. Olley

2002 Precision and Accuracy in the Optically Stimulated Luminescence Dating of Sedimentary Quartz: A Status Review. *Geochronometria* 21:1–16.

Murray, A., K. Thomsen, N. Masuda, J. Buylaert, and M. Jain

2012 Identifying Well-bleached Quartz Using the Different Bleaching Rates of Quartz and Feldspar Luminescence Signals. *Radiation Measurements* 47:688–695.

Ousley, Stephen

2013 ADBOU® 2.1.037. Software, available at http://math.mercyhurst.edu/~sousley/Software.

https://doi.org/10.7183/2326-3768.1.2.91 Published online by Cambridge University Press

Ousley, S., R. Jantz, and D. Fried
2009 Understanding Race and Human Variation: Why Forensic Anthropologists Are Good at Identifying Race. *American Journal of Physical Anthropology* 139(1):68–76.

Ousley, S.D., and R.L. Jantz
2005 FORDISC 3.0: Personal Computer Forensic Discriminant Functions. Department of Anthropology, University of Tennessee, Knoxville, TN.

Prescott, J. and J. Hutton
1988 Cosmic Ray and Gamma Ray Dosimetry for TL and ESR. *Radiation Measurements* 14:223–230.
1994 Cosmic Ray Contributions to Dose Rates for Luminescence and ESR Dating: Large Depths and Long-term Time Variations. *Radiation Measurements* 23:497–500.

Prideaux, G., G. Gully, A. Couzens, L. Ayliffe, N. Jankowski, Z. Jacobs, R. Roberts, J. Hellstrom, M. Gagan and L. Hatcher
2010 Timing and Dynamics of Late Pleistocene Mammal Extinctions in Southwestern Australia. *PNAS* 107(51):22157–22162.

Ramsthaler, F., K. Kreutz, and M.A. Verhoff
2007 Accuracy of Metric Sex Analysis of Skeletal Remains Using Fordisc ® Based on a Recent Skull Collection. *International Journal of Legal Medicine* 121:477–482.

Rhodes, E.
2011 Optically Stimulated Luminescence Dating of Sediments over the Past 200,000 Years. *Annual Review of Earth and Planetary Sciences* 39:461–488.

Rink, W.J., Dunbar, J.S., Tschinkel, W.R., Kwapich, S., Repp, A., Stanton, W., and D. K. Thulman
2013 Subterranean Transport and Deposition of Quartz by Ants in Sandy Sites Relevant to Age Overestimation in Optical Luminescence Dating. *Journal of Archaeological Science* 40(4):2217–2226.

Rittenour, T.
2008 Luminescence Dating of Fluvial Deposits: Applications to Geomorphic, Paleoseismic and Archeological Research. *Boreas* 37:613–635.

Roberts R., T. Flannery, L. Ayliffe, H. Yoshida, j. Olley, G. Prideaux, G. Laslett, A. Baynes, M. Smith, R. Jones, and B. Smith
2001 New Ages for the Last Australian Megafauna: Continent-wide Extinction about 46,000 Years Ago. *Science* 292:1888–1892.

Robinson, G., A. Wanek, W. Hays, and M. McCallum
1964 *Philmont Country: The Rocks and Landscape of a Famous New Mexico Ranch*. Geological Survey Professional Paper 505, United States Government Printing Office, Washington, D.C.

Rodnight, H.
2008 How Many Equivalent Dose Values Are Needed to Obtain a Reproducible Distribution? *Ancient TL* 26(1):3–9.

Sauer, Norman J.
1992 Forensic Anthropology and the Concept of Race: If Races Don't Exist, Why Are Forensic Anthropologists So Good at Identifying Them? *Social Science & Medicine* 34(2):107–111.

Sauer, Norman J. and Jane C. Wankmiller
2009 The Assessment of Ancestry and the Concept of Race in *Handbook of Forensic Archaeology and Anthropology*. World Archaeological Congress, edited by George Nicholas and Julie Hollowell, pp. 187–200. Left Coast Press, Walnut Creek, CA.

Schoeneberger, P.J., DA. Wysocki, E.C. Benham, and Soil Survey Staff.
2012 Field Book for Describing and Sampling Soils, Version 3.0, Natural Resources Conservation Service, National Soil Survey Center, Lincoln, Nebraska.

Scientific Working Group for Forensic Anthropology (SWGANTH)
2013 Ancestry Assessment. Electronic document, http://swganth.startlogic.com/Ancestry%20Assessment%20Rev0.pdf, accessed November 11, 2013.

Scott, G. Richard, and Christy G. Turner II
1988 Dental Anthropology. *Annual Review of Anthropology* 17:99–126.

Simmons, Virginia M.
2000 *The Ute Indians of Utah, Colorado, and New Mexico*. University Press of Colorado, Boulder.

Smithsonian Institution
2011 Osteoware® 2.4. Software, available at http://osteoware.si.edu.

Snow, Clyde C.
1982 Forensic Anthropology. *Annual Review of Anthropology* 11:97–131.

Suma, G.N., Balaji Rao, Rajeshwari Annigeri, Dayashankara RAo, and Sumit Goel
2011 Radiographic Correlation of Dental and Skeletal Age: Third Molar, an Age Indicator. *Journal of Forensic Dental Sciences* 3(1):14–18.

Tuan, Yi-Fu, Cyril E. Evard, Jerold G. Widdison, and Iven Bennett
1973 *The Climate of New Mexico*. Revised edition. New Mexico State Planning Office, Santa Fe.

Tuteja, Monica, Shraddha Bahirwani, and P. Balaji
2012 An Evaluation of Third Molar Eruption for Assessment of Chronological Age: A Panoramic Study. *Journal of Forensic Dental Sciences* 4(1):13–18.

Wallinga Jakob
2002 Optically stimulated luminescence dating of fluvial deposits: a review. *Boreas* 31(4):303–322.

Walker, P. L.
2008 Sexing Skulls Using Discriminant Function Analysis of Visually Assessed Traits. *American Journal of Physical Anthropology* 136:39–50.

Waters, M. S. Forman, T. Jennings, L. Nordt, S. Direse, J. Feinberg, J. Keene, J. Halligan, A. Lindquist, J. Pierson, C. Hallmark, M. Collings, and J. Wiederhold
2011 The Buttermilk Creek Complex and the Origins of Clovis at the Debra L. Friendkin Site, Texas. *Science* 331(6024):1599–1603.

Waters, M., S. Forman, T. Stafford, and J. Foss
2009 Geoarchaeological Investigations at the Topper and Big Pine Tree Sites, Allendale County, South Carolina. *Journal of Archaeological Science* 36:1300–1311.

White, Tim D. and Pieter A. Folkens
2005 *The Human Bone Manual*. Academic Press, New York.

Wintle, A., and S. Murray
2006 A Review of Quartz Optically Stimulated Luminescence Characteristics and Their Relevance in Single-aliquot Regeneration Dating Protocols. *Radiation Measurements* 41:369–391.

Authors

Warren K. Lail, **David Sammeth**, and **Jason Nevins** ■ New Mexico Highlands University

Shannon Mahan ■ US Geological Survey

https://doi.org/10.7183/2326-3768.1.2.91 Published online by Cambridge University Press

Only one archaeological survey tool can give you all this!

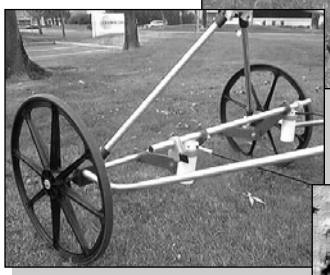
The G-858 MagMapper™ offers superior speed, reliability and ease of use for all magnetometer survey projects, but that's not all.

It also serves as a digital data acquisition system for the Geometrics OhmMapper™ capacitively coupled resistivity (CCR) system, the Geonics EM61, and integrates seamlessly with a GPS for a complete, multi-parameter mapping system, for the fastest, easiest, and most diagnostic archaeological surveys. Our mapping and interpretation software turns your PC into a personal interactive geophysical workstation.

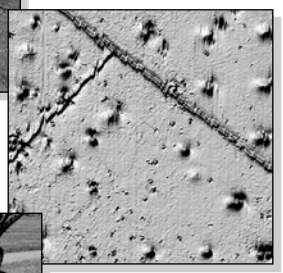
For archaeology, UXO surveys, hazardous waste, utility locating, and void detection, there's no better combination than the MagMapper™ system. ***Great plotting and modeling software and valuable case histories are available free on our website.***



Cesium magnetometer integrated with GPS for efficient data collection.



Nonmagnetic MagCart ™ for 1 to 5 sensors improves data quality & target analysis for precise mapping of sites.



MagPick™ software offers profile analysis and calculation of depth to target.

OhmMapper non-contact resistivity system. Fast, easy resistivity without stakes.



GEOMETRICS *Since 1969*

2190 Fortune Drive • San Jose, CA 95131 • U.S.A.
(408) 954-0522 • FAX: (408) 954-0902
E-mail: sales@mail.geometrics.com • www.geometrics.com

https://doi.org/10.7183/2326-3768.1.2.91 Published online by Cambridge University Press